Eur. Phys. J. D **15**, 87–97 (2001)

THE EUROPEAN PHYSICAL JOURNAL D

EDP Sciences
© Società Italiana di Fisica
Springer-Verlag 2001

An experimental confirmation of longitudinal electrodynamic forces

N. Graneau[1,a], T. Phipps Jr[2], and D. Roscoe[3]

[1] Dept. of Engineering Science, Oxford University, Oxford OX1 3PJ, England
[2] 908 South Busey Ave. Urbana, Illinois 61801, USA
[3] School of Mathematics, Sheffield University, P.O. Box 597, Sheffield S10 2UN, England

Received 15 November 2000 and Received in final form 12 March 2001

Abstract. According to the conventional views of electromagnetic theory, as these are expressed in the Lorentz force law, all the forces which act on a current carrying metallic conductor are perpendicular to the current streamlines. However, over the years, from Ampère through Maxwell until the present day, there have been persistent claims that when current flows in a metallic conductor, there are mechanical forces acting along current streamlines which subject the conductor to tensile stress, and which are therefore capable of performing work in the direction of current flow. The problem of substantiating these claims has always lain in the difficulty of designing an experiment in which the effects are unambiguously demonstrated. The present paper describes an experiment which to a large extent removes these ambiguities, and which provides a compelling novel demonstration of forces acting along current streamlines. A force calculation based on Ampère's original electrodynamic force law is found to be consistent with the observed behaviour.

PACS. 01.55.+b General physics – 03.50.De Classical electromagnetism, Maxwell equations – 41.20.-q Applied classical electromagnetism

1 Introduction

The claim for the existence of mechanical forces along current streamlines in metallic conductors has a history which stretches back to Ampère in the early 19th century and to experiments performed by him which involved U-shaped conductors floating in mercury baths being propelled by, what he claimed to be, forces acting in the direction of current flow. Maxwell was confronted with the problem of choosing between the Biot-Savart force law (now known as the Lorentz force law) and the law bequeathed by Ampère. In the absence of any discernible practical difference in their predictions, given the experimental equipment available in the 19th century, he expressed a preference for Ampère's law because it conformed with Newton's Third Law. However he still championed the Biot-Savart law, simply because it was expressed in terms of electromagnetic fields which were the speculative cornerstone of his treatise [1].

The claims next surfaced (in a very subdued way) in the early 20th century, when Hering, an American engineer, [2] designed a liquid metal pump which used the claimed existence of Ampèrian forces to pump liquid metal along current streamlines without the use of an externally applied magnetic field. This pump was sold commercially to the metal refining industry for a few years until a changing technology made it obsolete.

The matter seems to have rested there until the mid-1960's when a Polish physicist, Nasilowski [3] discovered that when a copper wire passed an overdamped pulsed current in a certain energy range, the wire "exploded" leaving a collection of wire fragments of undiminished diameter with fracture faces which were nearly perpendicular to the wire axis. Detailed metallurgical examination of the wire pieces revealed that the breaks were all caused by tensile fracture. These experiments, and a range of similar ones were repeated by Graneau [4, 5, 6a] at MIT in the 1980's and similar conclusions were drawn. As a response to the renewal of claims for the existence of the Ampère force, originating from Graneau and others [7–10], Robson and Sethian [11] (R&S) performed an experiment which they designed to test for the existence of such forces. Their experiment consisted of a fixed and rigid open circuit containing a mobile element separated from the main part of the circuit by air-gaps. The idea was that if two arcs bridged the air gaps between the main circuit and the mobile element so that a substantial current flowed through the circuit, then Ampèrian-type forces would manifest themselves as a motion of the mobile element in the direction of current flow. An analysis based on the presumption of the reality of the Ampère force shows that the mobile element cannot move if the fixed circuit is

[a] e-mail: neal.graneau@eng.ox.ac.uk

symmetric with respect to the centre-point of the mobile element, consequently R&S built their circuit to be asymmetrical in this sense. Their experiment was performed, and the mobile element did not move. R&S subsequently claimed that this proved conclusively that Ampèrian longitudinal forces were a fiction, and that the Lorentz force law was therefore unchallenged.

However, one of us (Phipps) [12,13] has pointed out that, whilst it is true that the circuit must be asymmetrical for the proposed Ampèrian forces to become apparent, an even more critical asymmetry lies in the length of the air gaps at each end of the mobile element. As a result, the shape asymmetry of the fixed metallic parts of the circuit with respect to the mobile element is of no consequence. The R&S experiment however, used only symmetric air gaps at each end of the mobile element and it was for this reason, Phipps argued, that R&S failed to observe a positive result.

The experiment described here, and performed by one of us (Graneau), corrects this deficiency in the R&S design and gives the very clear and unambiguous result that work is performed on the mobile element when current flows in the circuit with asymmetrical gaps. It is shown that the behaviour of these forces, under various current conditions, is satisfactorily modelled by the original electrodynamic force law, proposed by Ampère in 1822.

2 Qualitative description of the effect

The general claim is that when a current flows in a metallic conductor, then mechanical forces are created between pairs of current elements, and that these elemental forces, $\Delta F_{m,n}$, are described by Ampère's force law [4–6], which has the general form

$$\Delta F_{m,n} = -k\frac{i_m i_n \mathrm{d}m\mathrm{d}n}{r_{m,n}^2}, \tag{1}$$

where i_m and i_n are the currents flowing in the current elements of length $\mathrm{d}m$ and $\mathrm{d}n$ respectively, $r_{m,n}$ is the distance between the centres of the two elements (which can have finite size), and k is a dimensionless geometrical function that takes into account the direction of current in each element. The force between these elements is either a mutual attraction or repulsion acting along the line joining them, thus complying with Newton's third law. Ampère defined his current element as an infinitesimally small portion of a metal conductor and in this paper it is taken to be capable of being analysed ultimately as the individual metallic atoms of which the conductor is composed. This definition is in striking contrast to the modern current element which was defined by Lorentz as a free charged particle in motion.

When the physical structure consists of two independent, mechanically decoupled circuits, then the predictions of the Ampère force law concerning the force exerted by each circuit on the other are identical to the corresponding predictions of the Lorentz force law. This fact was well-known to Maxwell (to whom the magnetic component of the Lorentz law was then known as the Grassmann or Biot-Savart law) and it arises simply because the Ampère and Lorentz laws differ by an exact differential. If C_1 and C_2 are two independent circuits, the force exerted by C_1 on any given small segment of C_2 is found by integrating around the whole of the circuit C_1, and it is in this process of "whole circuit integration" that the exact differential difference between the two laws disappears.

This result has been used by R&S [11] and others [14–16] to suggest that the two laws are identical. However, apart from this coincidence, the two laws could not be more different. The Lorentz law predicts forces between pairs of current elements that do not conform to Newton's third law, implying that the magnetic field is required to absorb or emit momentum in order to retain the principle of momentum conservation. On the other hand, the Ampère law is a classical inverse square, instantaneous action-at-a-distance law, which does conform to Newton's third law between every pair of current elements, and thus does not require a magnetic field. Maxwell had no way of distinguishing empirically between the two laws. He preferred the Ampère law for its Newtonian provenance, but finally settled for the Biot-Savart law because it could be expressed in terms more compatible with Faraday's field concepts, of which he was a self-proclaimed advocate.

While this difference in fundamental structure between the two laws does not matter when considering the forces acting between two independent circuits, it leads to a crucial difference when considering the mechanical forces and stresses created within a single circuit due to its own current. Suppose we have a circuit, C, and want to compute the force exerted between a small section of this circuit, ΔC, and the rest of the circuit C' ($C' = C - \Delta C$). To apply the Lorentz law to this situation, it is first necessary to integrate around the whole of C in order to compute the magnetic field, and only then can the force exerted by this field on the conductor, ΔC, be computed. Now to apply the Ampère law to the situation correctly we must first recognize that, since it is a Newtonian force law, it must be applied in a manner consistent with the principles of Newtonian mechanics. One of these principles is that forces between objects within a closed system cannot affect the motion of that system. In the present example, the circuit element, ΔC, can be construed as a closed system so that, when computing the external forces felt by ΔC, the interactions between elements both in ΔC itself need not be included, since the resulting forces, while capable of producing internal tensions, cannot give rise to any net acceleration of ΔC itself.

In other words, whereas the application of the Lorentz law requires an integration around the whole of C in order to compute the magnetic force acting on ΔC, the Ampère law only requires integration around the external partial circuit C' in order to calculate the net force of attraction or repulsion between the two sections. The net effect is that in the proper application of Ampère's law, the difference between the two laws, which is expressed by an exact differential quantity, no longer disappears since there is no

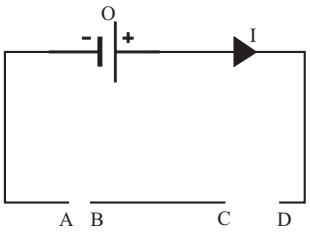

Fig. 1. Circuit used to demonstrate the importance of unequal air gaps in producing longitudinal motion.

closed loop integral, and the two laws therefore give rise to quite distinct predictions for this single-circuit circumstance. Further, the Ampère force law, unlike the Lorentz law, allows the possibility of calculating the Newtonian force of attraction or repulsion between any two arbitrary circuit sections.

In order to arrive at an experimental design potentially capable of distinguishing between the two laws, it is sufficient to note that the Lorentz law predicts that two collinear elements, pointing in the same direction, have no force between them, whereas the Ampère law predicts that two such elements repel each other [4, 5a, 6a]. This stark difference between the two laws leads to the idealised experimental design of Figure 1.

In this circuit, there are two sections: (a) the stationary part of the circuit, labelled AOD, which is assumed to be mechanically rigid and fixed to the laboratory; and (b) a mobile test element, labelled BC, which is free to move only along an axis which is parallel to the direction of current flow. The two conductor sections are mechanically decoupled, but are considered to be electrically coupled by spark gaps across AB and CD. The question to be considered is whether an arrangement of this circuit exists such that, when current flows, there is a force between the mobile test element and the fixed circuit, causing the element to accelerate along its axis.

Given the "inverse distance squared" nature of the Ampère force, it is obvious that if Newtonian longitudinal repulsive forces exist between BC and the fixed circuit, then they largely arise in those parts of the fixed circuit which are very near to points A and D. It follows immediately that if the mobile test piece is initially placed so that the gaps AB and CD are equal, then no motion of the test piece is likely to be observed when the current flows. In this case, the repulsion from the current elements near A will be cancelled by the equal and opposite repulsion from those near D. This "no motion" arrangement was precisely the one chosen by R&S [11] for their experiment and is the reason why we consider their experimental design to be flawed. Thus any experiment of this type which tests for relative longitudinal acceleration between BC and the rest of the circuit, must be arranged so that the gaps AB and CD are unequal.

The repulsive forces between the mobile element and the plasma in the arc gaps should be comparable or even greater than the forces between the element and the fixed circuit. However in this case the acceleration is almost completely acquired by the plasma simply because it has much less mass than the metallic element. Therefore any observed acceleration of the armature is purely a result of the repulsion between the element and the fixed circuit.

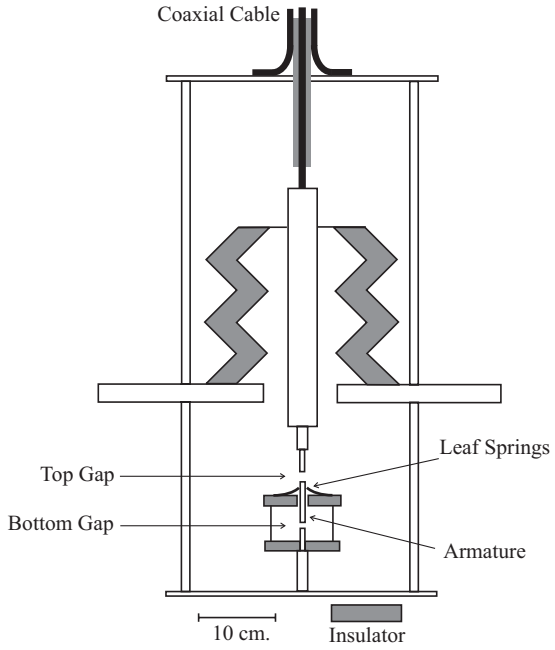

Fig. 2. Schematic description of the cylindrically symmetric experimental circuit, drawn to scale and showing only two of the six supporting legs.

Such Newtonian analysis, while still employed in the solution of mechanical problems, is no longer applied to modern electromagnetism as a result of the disuse of Newton's laws in relativistic field theory. However it is crucial that one applies Ampère's law in the Newtonian manner in which it was derived for only then will it make useful predictions.

3 Experimental details

3.1 Experimental design

A sketch of the mobile element part of our experimental circuit is shown in Figure 2. The basic test-bed consists of three metallic disks mounted coaxially above one another on six copper rods, each of total length 659 mm, which pass through six symmetrically arranged holes drilled 150 mm from the centre of each disc. The bottom and top disks are each of 350 mm diameter and 6 mm thick, and are fabricated in copper, whilst the central disk, which is arranged 254 mm above the bottom disk, is 530 mm diameter and 1″ thick, and is made of aluminium.

A high voltage coaxial cable enters the test-bed at the top, and the outer braid of this cable is clamped to the upper surface of the top disk, so that the whole disk/rod arrangement is conductively connected to this outer braid. The insulated inner conductor of the cable passes through a hole in the centre of the top disk and is then fixed to

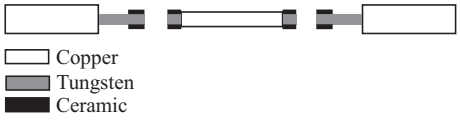

Fig. 3. Details of armature and electrodes.

a central high voltage insulating feed-through in the central disk. The bottom side of this conductor terminates in a 3/16″ diameter tungsten rod electrode, collinear with the central axis and 2 cm long. The squared off end of this upper electrode is arranged to be 75.5 mm above a similarly designed second electrode fixed rigidly into the bottom disk. The portion of the circuit, termed the mobile "armature", is coaxially supported in this 75.5 mm gap in a perspex frame, designed to prevent lateral and downward armature movement, but allowing it to move upwards. This constraint on the vertical motions is achieved by using two leaf-springs, arranged as in Figure 2, which provide very small resistance to upward armature motion, but a very large resistance to downward motion. This arrangement makes any upward displacement of the armature easily detectable since, if the armature does undergo any upward motion, it cannot thereafter fall down, allowing the height gained to be measured.

The armature consisted of a 45 mm length of 1/4″ diameter copper rod with 3/16″ diameter tungsten rod inserts extending 5 mm from either end of the copper rod. This gave a total armature length of 55 mm, and weighed 17.7 gm. To ensure that the arc current passed entirely through the end faces of the tungsten electrodes, the sides of these electrodes were coated with a quick drying ceramic insulation. This precaution enabled us to more accurately model the current as consisting of longitudinal streamlines near the arc gap regions. The ceramic was also applied to the stationary electrodes in the same manner. The arc electrodes are shown in detail in Figure 3. For two special cases to be described later, the copper-tungsten armature was replaced by a geometrically similar aluminium rod, and then later by a thin walled brass tube.

Finally, the coaxial cable was connected to a 50 kV capacitor bank, comprised of six, 1.67 μF capacitors in parallel. The circuit was switched by a pressurised triggered spark gap, and the total inductance was measured to be 2.8 μH.

3.2 Experimental results

The capacitor bank was charged to 33 kV for all of the reported shots. Various values of capacitance between 3.3–10 μF were selected by connecting the required number of capacitors in parallel. To eliminate the possibility that anode/cathode asymmetry effects may be responsible for the observed behaviour, for every shot performed with the bank charged positively, an otherwise identical shot was performed with the capacitors charged negatively. The bank was discharged *via* an air pressurised triggered spark gap, and the resulting current was measured with an integrating current transformer connected to a digital oscilloscope. All of the current traces were underdamped ringing waveforms. From these waveforms it was possible to measure the maximum current, the ringing frequency and the time constant of the decay.

The shots were performed with three distinct arrangements for the initial copper armature position, and two other experiments performed, one with an aluminium rod armature and the other with a brass tube armature. These different situations can be classified as described below:

(i) the copper-tungsten armature was initially placed resting on the lower electrode, so that there was a 20.5 mm air gap between the armature and the upper electrode;
(ii) the copper-tungsten armature was initially placed with air gaps of between 1–8 mm between it and the bottom electrode;
(iii) the copper-tungsten armature was replaced by an aluminium armature of the same length and diameter as the original one which was then soldered to the lower electrode in order to eliminate the lower arc. The aluminium-solder-copper bond ensures good electrical conductivity, but is mechanically weak and easily broken;
(iv) a brass tube of the same length and diameter as the original armature but with a 0.2 mm wall thickness, was initially placed resting on the lower electrode as in case (i);
(v) the original copper-tungsten armature was initially placed midway between the top and bottom electrodes so that the two air gaps were equal.

In cases (i), (ii), (iii) and (iv), after the discharge, the armature was found to have moved upwards by an easily measurable amount, whilst for the case (v), there was no detectable armature motion. This last result was as expected from the earlier discussion.

3.3 Discussion of the qualitative observations

The positive results of upward armature motion for the cases (i), (ii), (iii) and (iv) provide evidence for the existence of forces acting on the armature in the direction of current flow when the arc gaps at either end of the armature are unequal, whilst the case (v) is consistent with the absence of a net force when the arc gaps are of equal length.

The question is, "what is the origin of these forces?" There are two clear choices: either the forces have an electrodynamic origin, or they do not. Any claim that these forces are electrodynamic in origin is controversial since, according to the conventional view, all such forces are described by the Lorentz force law which declares that there are no forces acting in the direction of current streamlines. Further, since the circuit shape and dimensions are independent of the existence or relative lengths of the air gaps then it follows that the Lorentz law prediction is insensitive to the critical role of the air gaps since it involves a closed loop integration of the circuit in order to calculate the magnetic field acting on the armature. Consequently,

to claim that the observed forces depend on the relative lengths of the air gaps and have an electrodynamic origin is to claim that the Lorentz force law is not applicable to the physical situation being considered. Since such a view represents an attack on one of the foundations of modern physics, it is necessary to consider very carefully all conceivable mechanisms by which the armature could be accelerated in the observed manner within the context of the given experimental design.

The only non-electrodynamic forces that would be capable of accelerating the macroscopic armature can be broken down into three categories (1) gravitational forces, (2) mechanical forces and (3) electrostatic forces.

(1) *Gravitational forces*
We can exclude the effects of gravitational forces as a possible cause for the observed effects for two reasons. Firstly, these forces would be unaffected by the electrical discharge and it is quite clear that the observed armature acceleration only occurs when high current pulses are passed around the circuit. Secondly, gravitational forces could only pull the armature down toward the earth, while in the experiment the armature is always observed to move upwards.

(2) *Mechanical forces*
The possibility of armature acceleration by mechanical forces must be carefully investigated. Such forces could be of two types, either thermal expansion of the arc plasma colliding with the armature or explosive ablation of material away from the electrode end faces. The magnitude of these forces is difficult to estimate theoretically as a result of many unknown arc and electrode parameters. Thus qualitative tests were performed to examine the plausibility of these mechanisms. In the case (i) and (iii) shots during which the armature was initially resting on the bottom electrode, there were absolutely no signs of arc-ablation on the surface of the bottom electrode or the bottom surface of the armature. By contrast, for these shots, there was considerable evidence of arc ablation on the surface of the top electrode and the top surface of the armature. The absence of arc ablation on the two bottom surfaces was then interpreted as a positive indication of the absence of arcing at all between these surfaces, and yet this was the area from which the armature moved away. It is therefore clear that the armature is not accelerated upward by mechanical arc forces. One can also draw the conclusion that current only flowed whilst the armature and bottom electrode were in good electrical contact. It follows that the actual armature motion occurred after the current pulse had terminated. This knowledge later enabled us to model the force as an impulse which had stopped acting before the armature had moved significantly.

(3) *Electrostatic forces*
There will be electrostatic forces that develop between the end faces of the electrodes during the period when the full capacitor voltage is impressed on them but before the air gaps break down to form arcs. Further there are several mechanisms which develop electrostatic fields during the breakdown and AC current phase. In order to examine these forces we must look separately at the two different experimental situations which are distinguished by (a) the armature initially being electrically isolated from the fixed electrodes by a lower and upper gap, cases (ii), (v) and (b) a single air gap with the armature initially resting on the lower electrode, cases (i), (iii) and (iv).

In the first situation (a), simple electrostatic considerations reveal that even though the electrically isolated armature may become polarised by an electrostatic field, there can be no net electrostatic force on an isolated charge neutral object. Therefore in the case (ii) experiments, pre-breakdown electrostatic forces cannot be the cause of the observed upward acceleration.

In the situation (b) for which the armature is initially resting on the bottom electrode, there are three mechanisms that create electrostatic fields between the electrodes and the armature. The most significant is the pre-breakdown attractive electrostatic force created between the top of the armature and the upper electrode which can be expressed as [17]

$$F = -\frac{\varepsilon_0 A V^2}{2d^2}, \tag{2}$$

where ε_0 is the permittivity of free space ($\varepsilon_0 = 8.85 \times 10^{-12}$ F/m), A is the cross-sectional area of the electrode and armature end faces ($A = 1.8 \times 10^{-5}$ m^2), V is the voltage between the two fixed electrodes ($V = \pm 33$ kV) and d is the length of the upper gap ($d = 0.02$ m). A negative force represents attraction and thus equation (2) predicts an upward force on the armature.

The moment of arc breakdown was indistinguishable from the time that the trigger button was depressed. Nevertheless being generous, it is possible to say that the electrostatic force may have been impressed on the armature for a period of up to 1 second even though it was probably several orders of magnitude lower than this. If we call this period Δt ($\Delta t \leq 1$ s), then a maximum upward electrostatic impulse on the armature can be calculated as

$$F\Delta t\,(\text{electrostatic}) = \frac{\varepsilon_0\, A V^2 \Delta t}{2d^2} \leq 2.2 \times 10^{-4}\ \text{Ns}. \tag{3}$$

An upward impulsive force will cause the armature to rise a distance, h. By measuring h, the initial momentum mv_i of the armature can be calculated by equating the initial kinetic energy of the armature ($mv_i^2/2$) to the potential energy (mgh) it has gained at the top of its rise. With neglect of friction losses

$$mv_i = m\sqrt{2gh} = F\Delta t, \tag{4}$$

where g is the acceleration due to gravity. The 12th shot listed in Table 1 had no initial bottom gap and showed that the 17.7 gm armature was raised to a height of 11.0 mm. With equation (4), this yields

$$F\Delta t\,(\text{measured}) = 8.2 \times 10^{-3}\ \text{Ns}. \tag{5}$$

Comparison of equations (3) and (5) reveals that the measured impulses are at least an order of magnitude larger

Table 1. Experimental results (using ceramic sheathed, tungsten tipped electrodes).

					Initial gaps			
V_0 (kV)	C (μF)	I_0 (kA)	ω (rad/s)	$1/\alpha$ (μs)	top (mm)	bottom (mm)	h (mm)	k
+33	3.3	+42.9	3.4×10^5	54.3	20.0	0.0	2.5	1.57
+33	3.3	+42.9	3.4×10^5	54.3	20.0	0.0	2.5	1.57
+33	3.3	+42.9	3.4×10^5	54.3	19.3	1.0	3.0	1.72
+33	3.3	+42.9	3.4×10^5	54.3	18.2	2.0	1.9	1.37
+33	5.0	+54.6	2.8×10^5	66.2	20.2	0.0	4.1	1.02
−33	5.0	−51.7	2.8×10^5	70.9	20.5	0.0	4.0	1.05
+33	5.0	+54.6	2.8×10^5	66.2	19.1	1.0	10.3	1.61
−33	5.0	−51.5	2.8×10^5	69.6	19.5	1.0	5.8	1.29
+33	5.0	+53.1	2.8×10^5	65.3	18.1	2.0	4.1	1.09
−33	5.0	−51.9	2.8×10^5	64.9	18.5	2.0	3.3	1.03
+33	6.7	+62.3	2.5×10^5	73.5	20.0	0.0	8.9	1.04
−33	6.7	−61.8	2.5×10^5	75.9	20.5	0.0	11.0	1.13
+33	6.7	+62.4	2.5×10^5	71.9	19.3	1.0	16.0	1.42
+33	6.7	+60.9	2.5×10^5	69.0	18.3	2.0	8.4	1.12
−33	6.7	−60.3	2.4×10^5	75.1	18.5	2.0	6.6	0.93
+33	6.7	+63.5	2.5×10^5	67.1	16.3	4.0	1.3	0.42
+33	6.7	+63.5	2.5×10^5	63.7	15.5	5.0	1.0	0.39
−33	8.3	−68.7	2.2×10^5	78.9	17.5	3.0	11.5	0.90
+33	8.3	+71.2	2.2×10^5	68.0	16.3	4.0	2.8	0.48
+33	10.0	+75.0	2.0×10^5	81.3	16.3	4.0	3.3	0.39
+33	10.0	+76.5	2.0×10^5	74.6	12.3	8.0	0.6	0.18
+33	10.0	+76.5	2.0×10^5	74.6	10.2	10.2	0.0	0.00

mass of armature = 17.7 gm.

than those predicted by the pre-breakdown electrostatic forces.

The rapidly changing current levels as a result of the arc breakdown could potentially cause the generation of an induced electrokinetic field [18] across the arc gap which will have a maximum value at the first zero crossing of the arc current. However the current pulse only lasts for $\sim$150 μs. Using knowledge of the measured mechanical impulse from equation (5), we can use equation (2) to show that the required potential across the arc gap to give the observed motion is $\geq$ 21 MV. This corresponds to more than five orders of magnitude more energy than existed when the capacitor bank was originally charged to 33 kV and would have broken down the insulation in the cabling and destroyed the capacitors. Thus energy conservation precludes the existence of such an acceleration mechanism. Further, the measured potential drop across high power ($I > 1$ kA) copper/air arc gaps less than 40 mm long is almost zero [19] and will be similar for Tungsten electrodes. Consequently, electrostatic fields across the arc gaps during the discharge cannot explain the effects observed in cases (i), (iii) and (iv).

In cases (i), (iii) and (iv) the differing material properties (σ, conductivity and ε, permittivity) due to bad contact, solder and oxide layers could cause the creation of electrostatic fields across the interface where the armature is connected to the bottom electrode during the period of current flow [20]. These fields however cause attraction and therefore cannot explain the observation that the electrode and armature become separated by the current pulse.

As a result of these considerations, we can conclude that the experiments described here cannot be explained by electrostatic forces in either the pre or post breakdown periods.

Since there is no conceivable mechanism which could create an armature moving force *after* the current pulse, we are led to conclude that the force which caused the armature to move appeared to have been contemporaneous with the current. These considerations lend weight to the hypothesis that the forces which manifestly act in the described experiment have an electrodynamic origin.

3.4 Analysis of quantitative data

Since all alternative mechanisms have been shown to be unable to explain the observed phenomena, we will analyse the data in such a way so that we can compare it with the predictions of Ampère's force law. The magnitude of the longitudinal force component, F, acting on the armature, according to the Ampère force law, can be expressed in

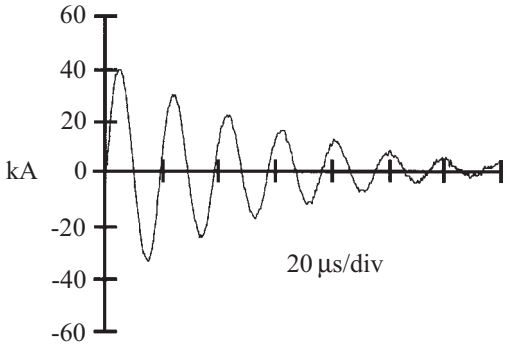

Fig. 4. A sample current waveform, taken from the first result in Table 1.

S.I. units as

$$F = \frac{\mu_0}{4\pi} k i^2 \tag{6}$$

for the described experimental circumstances, where k is the current-independent, dimensionless, Ampèrian force constant, which depends purely on the geometry of the circuit, μ_0 is the permeability of free space and i is the current. Consequently, since the time-integrated impulse gives the momentum gain in the system, we can write

$$mv_i = \int_{t=0}^{\infty} F \mathrm{d}t = \frac{\mu_0}{4\pi} k \int_{t=0}^{\infty} i^2 \mathrm{d}t, \tag{7}$$

where m is the armature mass. A typical current waveform produced by the power supply is illustrated in Figure 4, and a curve of this type can be closely approximated by an exponentially decaying sinusoid, with frequency ω, and decay time constant $(1/\theta)$,

$$i = I_0 \exp(-\theta t) \sin(\omega t), \tag{8}$$

so that after integration, equation (7) can be approximately expressed as

$$mv_i = \frac{\mu_0}{4\pi} \frac{k I_0^2}{4\theta} \left(\frac{\omega^2}{\omega^2 + \theta^2} \right). \tag{9}$$

Use of equations (4, 9) now allows the Ampèrian force constant to be expressed as

$$k = \frac{16\pi\theta m\sqrt{2gh}}{\mu_0 I_0^2} \left(\frac{\omega^2 + \theta^2}{\omega^2} \right). \tag{10}$$

In practice, for our experiments $\omega \gg \theta$, and so the bracketed term of this last expression was always approximately unity. Thus the following analysis assumes the approximation

$$k = \frac{16\pi\theta m\sqrt{2gh}}{\mu_0 I_0^2}. \tag{11}$$

Since the armature mass, m, is known to be 17.7 gm, and since values of I_0 and θ can be estimated from the current waveform, and h is measured for each shot, then a dimensionless value of k can be measured for each shot. If the Ampèrian force law is appropriate for the given circumstances, then it is to be expected that theoretically calculated values of k will be approximately equal to those measured by using equation (11).

3.5 Summary of experimental results

Cases (i) and (ii). All shots performed under the conditions of these cases gave a range of k-values that were consistent with the hypothesis that k is a function of the asymmetry of the air-gap lengths, and the details are discussed in the following sections.

Case (v). This case, for which there were equal air-gaps above and below the armature, resulted in no armature movement. This was expected and is consistent with the R&S [11] results. The net force predicted in this geometry is zero (*i.e.* $k = 0$).

Case (iii). It has already been observed how the absence of arc-ablation on the bottom electrode/armature surfaces for the case (i) shots indicates that arc pressure is not required for upward armature movement. However it was felt that a more convincing demonstration was required. To provide such proof, the copper armature was replaced by a solid aluminium armature, of the same length and diameter as the copper one. It was soldered to a copper bottom electrode, knowing that an aluminium-solder-copper bond is mechanically weak. When the capacitor bank was discharged through the circuit the solder joint was broken and the armature was displaced upwards by a considerable amount. Subsequent inspection showed that the solder had not been ablated and remained continuous across the interface. This case therefore provides very convincing evidence for the existence of strong vertical forces without the help of arc pressure. Since a lot of the available impulse was expended in breaking the solder bond, this case could not be used to make measurements of k.

Case (iv). Even though the skin effect should restrict the current to a thin layer on the outer surface of the armature, the brass tube armature was used to categorically remove the possibility of the existence of any radial currents in the armature. The tube was 55 mm long, $1/4''$ diameter, 0.2 mm wall thickness, and the first 5 mm of the inside and outside surfaces at both ends of the tube were coated with the quick drying ceramic previously described. As a result, current could enter or leave the tube only *via* the thin annular end faces. By eliminating radial currents and still observing strong upward forces, it can be claimed that the Lorentz force law cannot predict the motion observed.

Quantitative results from cases (i), (ii) and (v) are shown in Table 1.

4 Theoretical modelling of the system

4.1 Ampère's force law

From the results presented above, we can say that there is a force on the armature in the direction of, or directly opposed to, current flow. This force also appears to be independent of the direction of current flow. It has been shown in Section 3.3 that the observed forces could only be caused by electrodynamic longitudinal forces. Such forces can never be predicted by the Lorentz force law, so the

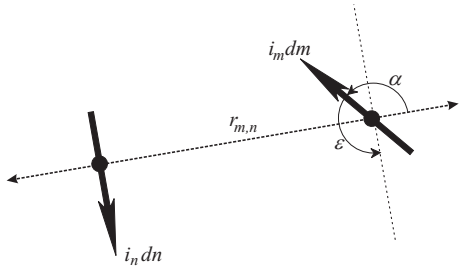

Fig. 5. Geometrical parameters used in Ampère's force formula, equation (12).

question arises, "to what extent is the observed effect consistent with quantitative predictions made by the Ampère force model?"

In S.I. units, the Ampère force between two current elements $i_m \mathrm{d}m$ and $i_n \mathrm{d}n$ can be written as:

$$\Delta F_{m,n} = -\frac{\mu_0}{4\pi} \frac{i_m i_n \mathrm{d}m \mathrm{d}n}{r_{m,n}^2} (0.5 \cos\varepsilon - 1.5 \cos(2\alpha + \varepsilon)), \tag{12}$$

where the i_m and i_n again represent the current in the elements of length $\mathrm{d}m$ and $\mathrm{d}n$ respectively and $r_{m,n}$ is the distance separating the centres of the two elements. α is the angle through which one has to rotate the line of action between the two elements to line up with the direction of the current in, say, element $\mathrm{d}m$, whilst ε is the angle through which one has to rotate the chosen element to line up with the direction of the other element, $\mathrm{d}n$. The angles α and ε have to be measured in the same rotational sense. These element parameters are shown in Figure 5. A positive force represents repulsion and conversely attraction is predicted by a negative force. As an important detail, Ampère showed that his law only describes the interaction between co-planar resolutions of element pairs. To make this claim, he used a symmetry argument to show that the resolution of one element in a direction orthogonal to the plane containing the other element and the distance vector that connects the two elements led to a zero force interaction between them. Also since real current elements must be volume elements, and yet are characterised by a 1-dimensional length, they can be modelled as a sphere or a cube. These considerations are more completely presented in [5b, 6b]. In the calculations presented here, cubic elements are used so that the conductor volume can be completely filled.

4.2 Circuit simplifications for modelling purposes

Practical realities make it extremely difficult to model in detail the actual circuits built for experimental demonstrations, and so it is necessary to make judicious simplifying assumptions about such circuits before they can be analysed. For the purposes of calculating the amount of work performed by the armature as a result of forces determined by Ampère's force law, these assumptions are listed below.

Assumption 1. Apart from the moving armature, the circuit consists of two distinct parts: (a) the fixed metallic part; and (b) the arc gaps. The current flowing in each of these two parts will give a component of force acting on the armature. However, it must be remembered that the mass of the fixed circuit is many orders of magnitude greater than the mass of the armature which in turn is many orders of magnitude more massive than the arc plasma. As a result, it is possible to argue from elementary momentum considerations that the observable work performed on the armature as a result of the forces caused by the arc plasma is negligible compared to the observable work caused by the armature's interaction with the metallic part of the circuit [21]. For this reason, the simulation ignores the interactions between the armature and the plasma. Finally, since the only present concern is to calculate those forces which cause the armature to move, and since we are assuming Newtonian physics, it is also not necessary to calculate those stresses in the armature which arise purely from internal element interactions.

Assumption 2. The true circuit shape was not entered into the model because of complications such as the non-uniform cross-section of the central conductor and the lack of knowledge of the current streamlines in the upper and lower copper disks. The coaxial cable was ignored because of the close proximity of current flowing in opposite directions in the cable, leading to negligible net interaction with the armature. Similarly, the capacitors and the switch circuitry were considered sufficiently distant from the armature to be ignored. The calculation subsequently showed that 75% of the force on the armature is due to the nearest 5 cm of the fixed conductor, thereby justifying the neglect of the effects of the capacitors, switch and coaxial cable.

Assumption 3. The circuit was considered to be equivalent to that obtained by taking six identical rectangular conducting frames arranged, firstly, so that one of the long sides of each is slotted into a common central conductor, and secondly, so that in the plan view, the six rectangular frames are seen to be symmetrically displaced with respect to the common central conducting axis. This central axis contains the mobile armature and arc gaps. With this arrangement, if the current in the central conductor is I, then the current in each of the six peripheral legs of the circuit is $I/6$. As a result, the longitudinal Ampère force on the armature (current I) due to its interaction with any of the peripheral legs (current $I/6$) will be proportional to the product of the two currents $I^2/6$. Consequently, the total longitudinal Ampère force on the armature due to its interaction with all six peripheral circuit legs is proportional to $(6 \times I^2/6 = I^2)$. Thus an equivalent circuit for predicting the axial forces on the armature is a single rectangle passing a current I, as shown in Figure 6, which is the circuit used in the computational model. It is to be noted that the axial symmetry of the *real* circuit means that there can be no transverse forces acting on the armature, and that is true independently of which force law one assumes. However, since this is manifestly not true of the model circuit, then this circuit can only be assumed

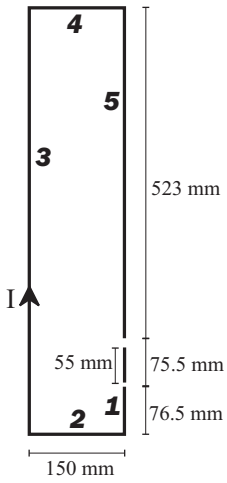

Fig. 6. Schematic description of the circuit used for the Ampère force calculation, showing the labels describing the circuit sections as used in Table 2.

useful for the explicit purpose of calculating longitudinal force distributions.

Assumption 4. The actual electrode and armature tips were of $3/16''$ diameter circular cross-section. As a result $3/16''$ square cross-section conductors throughout the entire circuit have been assumed, which greatly simplifies the finite element modelling process.

4.3 Calculation results

The conductor was split into a number of square cross-section filaments, N, containing cubic volume current elements. Thus the width of the filaments determines the length of the elements and thus the number of elements in the circuit. As the number of filaments increases, the force on the armature is found to decrease slightly. This has been previously interpreted in Graneau [5b, 6b, 22] as representing the actual force when the element size approaches the inter-ionic or metal lattice spacing, which corresponds to approximately 3×10^{14} filaments. It is impossible to compute with such a large number of element interactions, and in fact we were only able to use $N = 1$, 4, 9, 16, 25, 36, 49 and 64 filaments for calculations performed on a personal computer. Investigation of the Ampère force between two small conductor sections, using up to 900 filaments, has shown that the calculated dimensionless Ampère force constant, $k'(N)$, is related to the number of filaments by the empirically deduced equation:

$$k'(N) = k + \frac{Z}{N}, \tag{13}$$

where Z is a constant. Since in reality $N = 3 \times 10^{14}$, then k can be considered to be the calculated Ampère force, which can be compared to the measured k in equation (11). The calculated forces, $k'(N)$, were thus plotted against $1/N$ in order to determine k by linear regression. The calculation was performed for bottom gaps between

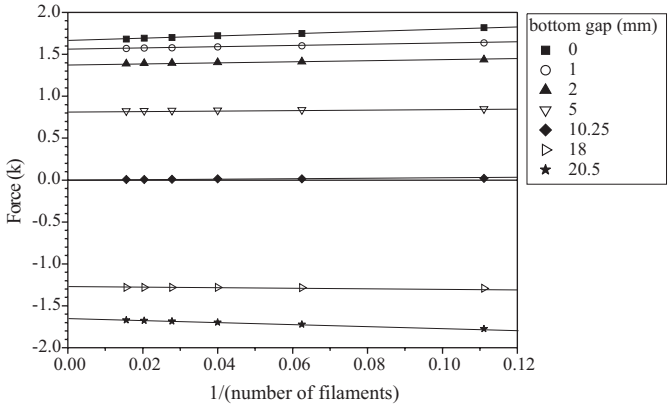

Fig. 7. Convergence calculation used to predict the Ampère force (k) for large numbers of filaments (N).

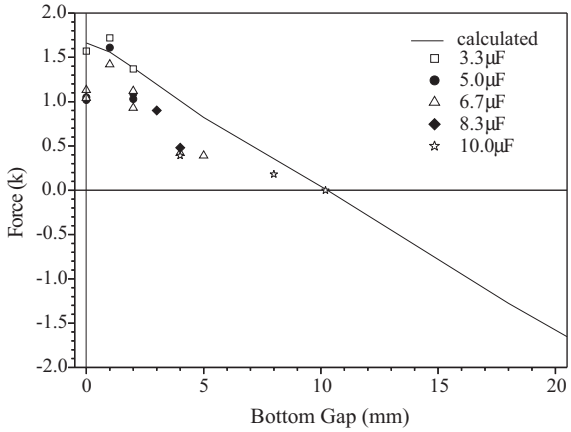

Fig. 8. Force (k) as a function of the initial bottom gap, showing the Ampère prediction and experimental data points.

electrode and armature of 0, 1, 2, 10.25, 18 and 20.5 mm, while keeping the sum of the two gaps equal to 20.5 mm. With only 1 and 4 filaments, the large element length in relation to the gap lengths made these calculations quite imprecise, and thus only the values for 9, 16, 25, 36, 49 and 64 filaments were used in the regression analysis shown in Figure 7. The resulting k values for 3×10^{14} filaments are shown as the complete curve in Figure 8, together with the experimentally measured values from Table 1. Positive k values represent an upward force, and the actual instantaneous total force values can be obtained by substituting k into equation (6).

It can be seen that the data points do not all lie directly on the curve. However, there is a good correspondence between experiment and the Ampère force prediction. Importantly, the force does go to zero at equal top and bottom gap lengths. This is the reason that R&S [11] observed no motion in their experiment. There is evidence that shots with lower capacitance, lower I_0, and lower $1/\theta$ time constant, gave consistently higher k values than the higher energy shots. This possibly implies that the current distribution on the electrode end faces is different for differing current strengths. Low current arcs usually attach to the cathode at a number of small high current

density spots, known as cathode spots, which are local hot regions, allowing easier electron emission. However at higher currents, there is more energy and larger sections of the surface of the cathode can become hot enough for good electron emission, and the current density thus becomes more uniform across the surface. The locally high current densities at the cathode spots, which are not included in the model, may explain why some of the lower current (lower capacitance) shots even lie above the predicted curve. The lower k values of the high current shots may also be the result of increased electrode ablation. The top gap, which was always the longer of the two, must have had a higher voltage drop across it, and post shot inspection revealed more erosion than at the bottom gap. Tungsten was chosen as the electrode material in order to minimize this effect. Nevertheless more ablated armature mass from the top armature surface than from the bottom would lead to a downward force component on the armature, which would be expected to increase with current. Friction between the armature and leaf springs has not been taken into account either, and its effect would be to lower the predicted forces by a small amount, leading to a better correspondence between theory and experiment than shown in Figure 8.

The impact of the skin effect has been explored, and it is found that if the current is allowed to flow only in the outer 0.3 mm of the conductor (which represents the skin depth in copper at 53 kHz (see Fig. 4)) then the overall predicted forces are reduced by roughly 9%, but the form of the curve remains the same. This again would pull the force prediction curve closer to the experimental data points. A more detailed skin effect calculation was not performed because keeping the same skin thickness while using different numbers of filaments requires more filaments than was practicable. Monte Carlo calculations [13], using a filamentary approximation, confirm these quantitative results both for the skin effect and for the full volume current flow as modelled in the main calculation described in this paper.

In order to demonstrate that the largest predicted forces on the armature are due to the current in the conductors nearest to it, we can show the total armature force broken down into its contributions as a result of interactions with five separate sections of the circuit. When current is flowing with constant density throughout the conductor cross-section, containing 64 filaments, the force on the armature can be broken down into contributions from each section of the circuit. If the sections are labelled as in Figure 6, the results are shown in Table 2. These results show clearly that the force on the armature is mainly due to its nearest conductors. This is why the geometrical length of the arc gaps, but not the arcs themselves, is so relevant to the determination of the acceleration of the armature.

5 Conclusions

An experiment has been performed which gave an unambiguous demonstration of the existence of a substantial force acting on a metallic conductor in the direction of current flowing through it. There were three questions to be answered:

(i) "Did this force have an electrodynamic origin?"
(ii) "If the force did have an electrodynamic origin, could the Lorentz force account for the observed work performed?"
(iii) "If the Lorentz force cannot account for the observed work, can the Newtonian based Ampère force account for this work?"

Table 2. Demonstration of the contribution to the total force on the armature from the five conductor sections shown in Figure 6. These numbers represent a 64 filament calculation with an even current density throughout the conductor cross-section with bottom and top gaps of 0.0 and 20.5 mm respectively.

Conductor section	Force contribution
1	2.4249
2	0.4608
3	0.0007
4	−0.0112
5	−1.1922
Total	1.6831

For the first question, there are three conceivable non-electrodynamic sources of force in the direction of armature motion. These are gravitational, mechanical and electrostatic mechanisms. It has been demonstrated in Section 3.3 that none of these is capable of explaining the observed armature accelerations, and therefore the force must be of electrodynamic origin.

For the second question, since the Lorentz force can only act at right angles to the flow of any current, this reduces the question to "was there any transverse flow of current in the armature?" One possibility for such radial currents would have been if the arc had attached itself to the sides of the armature, however this was prevented by the ceramic coating which only exposed the end faces to the arc. Another possibility for radial currents is current coming into the end face of the armature and then heading for the outer surfaces. However the brass tube armature precluded such currents and was still observed to move upwards. Moreover the dependence of the observed force on the relative lengths of the arc gaps demonstrates that the force is not caused by the magnetic field of the entire circuit, as calculated by the complete loop integral and required by the Lorentz law, which therefore cannot explain the experimental results.

For the third question, a numerical simulation of an idealised form of the circuit under the assumption of Ampère's force law has been performed. Subject to identifiable sources of energy losses (*e.g.* arc-ablation, friction etc.) and computational difficulties arising from the complexity of the problem (*e.g.* circuit shape and current distribution), it has been shown that the observed phenomena can be consistently described by this force law.

Finally, it should be recognised that, as a matter of historical fact, the Ampère force law has never been found in conflict with any experiment.

We would like to thank Dr. Peter Graneau for continuous input during the course of these and earlier Ampère force investigations and Peter Cambrook for his assistance in the performance of the experiment.

References

1. J.C. Maxwell, *A Treatise on Electricity and Magnetism* (Clarendon Press, Oxford, 1873), preface and articles 526, 687.
2. C. Hering, J. AIEE **42**, 139 (1923).
3. J. Nasilowski, in *Exploding Wires*, edited by W.G. Chase, H.K. Moore (Plenum, New York, 1964), Vol. 3, p. 295.
4. P. Graneau, Phys. Lett. A **97**, 253 (1983).
5. P. Graneau, *Ampère-Neumann Electrodynamics of Metals*, 2nd edn. (Hadronic Press, Palm Harbour FL, 1994), (a) chapter 2, (b) chapter 3.
6. P. Graneau, N. Graneau, *Newtonian Electrodynamics* (World Scientific, Singapore, 1996), (a) chapters 2, 5, (b) chapters 3, 4.
7. P.T. Pappas, Nuovo Cimento B **76**, 189 (1983).
8. J. Nasilowski, IEEE Trans. Mag. **20**, 2158 (1984).
9. T.E. Phipps, T.E. Phipps Jr, Phys. Lett. A **146**, 6 (1990).
10. R. Saumont, Phys. Lett. A **165**, 307 (1992).
11. A.E. Robson, J.D. Sethian, Am. J. Phys. **60**, 1111 (1992).
12. T.E. Phipps Jr, Apeiron **17**, 1 (1993).
13. T.E. Phipps Jr, Hadronic J. **19**, 273 (1996).
14. C. Christodoulides, J. Phys. A, Math. Gen. Phys. **20**, 2037 (1987).
15. D.C. Jolly, Phys. Lett. A **107**, 231 (1985).
16. J.G. Ternan, J. Appl. Phys. **57**, 1743 (1985).
17. W.J. Duffin, *Electricity and Magnetism*, 4th edn. (McGraw-Hill, 1990), p. 118.
18. O.D. Jefimenko, *Causality, Electromagnetic Induction and Gravitation* (Electret Scientific, Star City, W. Virginia, 1992), p. 29.
19. G.R. Jones, M.T.C. Fang, Rep. Prog. Phys. **43**, 1415 (1980).
20. O.D. Jefimenko, *Electricity and Magnetism* (Apple-Century-Crofts, New York, 1966), p. 296.
21. T.E. Phipps Jr, Phys. Essays **10**, 615 (1997).
22. N. Graneau, Phys. Lett. A **147**, 92 (1990).